scientific reports



OPEN

Development of a smart farming tool to monitor the degree of dew retting of flax stems

Ali Reda, Jean-Michel Mallet, Lionel Buchaillot & Steve Arscott[™]

Flax fibres are a natural, sustainable product which have applications ranging from textiles to composite materials. A process known as 'retting' is required to facilitate the mechanical extraction of flax fibres from their associated stems. The goal of retting is to break down the binding material (pectin) holding the fibre bundles to the core and epidermis of the stem, not the pectin which holds the single fibres together which form long, practical 'technical' fibres. For natural dew retting, there is therefore an optimum retting period: insufficient retting renders fibre extraction difficult and leads to low yield, whereas excessive retting can lead to poor technical fibre quality. For centuries, the timing of the retting termination has been evaluated by artisanal means. Today, modern technology enables one to envisage tools that indicate optimal retting. Here, we demonstrate the development of a smart tool combining mechanics, digital microscopy, and image analysis. The cracking of the outer tissue of the flax stems, due to mechanical torsion applied to the stems by the tool, is quantified using optical microscopy and image analysis, and is demonstrated to serve as an observable indicator of the degree of retting of the stems.

Keywords Flax fibre production, Optimal dew retting, Smart tool, Precision agriculture, Mechanical measurements, Image analysis

Flax fibre is a sustainable, natural bast fibre product which has widely-recognized attributes and numerous applications^{1,2}. In order to mechanically extract flax fibres from their parent stems in a factory, an initial process known as retting is required. Of the various retting approaches, dew retting is a natural biological process that involves the decomposition of the pectin and other binding substances, e.g. hemicelluloses and lignin, that hold the single fibres in bundles and the fibre bundles to the woody core (xylem) and the outer epidermis of the stem³⁻⁶. The specific goal of retting is to separate the fibre bundles, located near the surface of the stems, from the non-fibrous stem tissue without damaging them. Even though it has long been known that there is an optimal retting time, it is only relatively recently that the biological mechanism for an optimal dew retting was understood and described7. Under and over retting mainly affects the yield of what are known as 'technical fibres' (long bundles of relatively short, single fibres held together with pectin). Under retting results in fibre bundles which remain tightly attached to the woody core and the epidermis, making fibre separation during the mechanical extraction process difficult and yield lower. Over retting results in an excessive breakdown of the fibre bundles (due to degradation of the middle lamella between individual fibres). In this case mechanical extraction can result in the recuperation of technical fibres with less pectin and undesirable shorter, single fibres. In addition, excessive retting is thought to degrade the cellulose of single fibres, this can result in lower quality fibres⁸ in terms of technical fibre strength, cleanness and fineness, colour and lustre, and length³. The optimal retting stop-point has been judged for millennia⁴ using artisanal means which have been qualitatively described⁹. Various approaches (biological, chemical, physical, and imaging) have been investigated to develop a tool to measure the degree of retting and identify the optimal stop point^{8,10-15}. Of these, mechanical approaches appear to be promising as the goal of retting is to weaken the exterior of the stem sufficiently for optimal fibre

Here, we identify and study mechanically-induced surface cracking as an original observable to monitor the degree of dew retting in flax stems. By combining plant stem mechanical modelling, digital optical microscopy, and image analysis, we produce an original smart farming tool capable of predicting the optimal dew retting stopping point for optimal flax fibre extraction and quality. Figure 1 presents an overview of the methodology and main steps of the study.

Institut d'Electronique de Microélectronique et de Nanotechnologie (IEMN), Polytechnique Hauts-de-France, Centrale Lille, CNRS, University of Lille, Lille 59000, France. [™]email: steve.arscott@univ-lille.fr

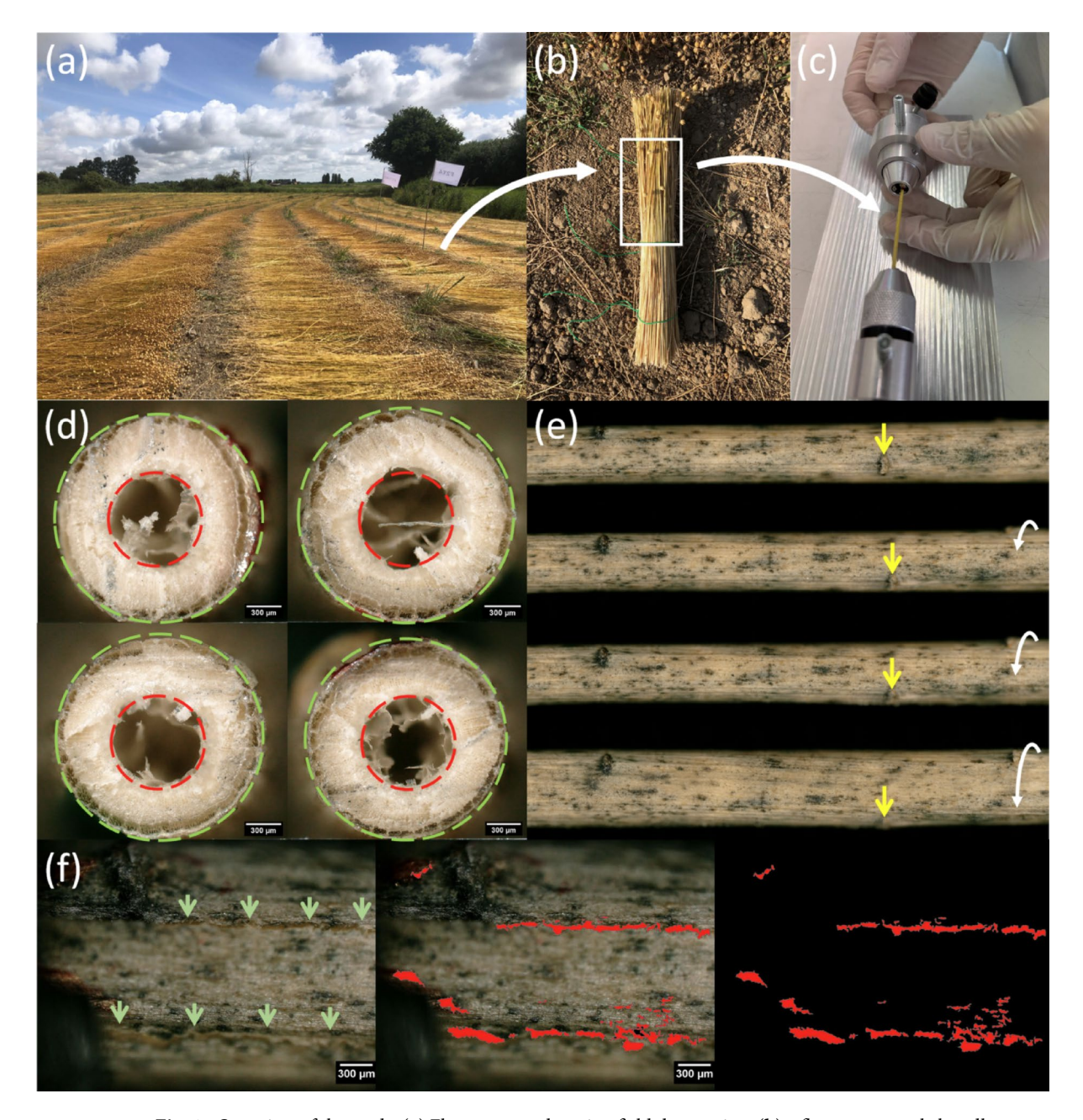


Fig. 1. Overview of the study. (a) Flax stems undergoing field dew retting, (b) a flax stem sample bundle collected for the experiments, (c) a flax stem sample mounted in the torsion tool, (d) optical microscope images of the cross section of flax stems: outer diameter (light green dashed circle) and inner diameter (red dashed circle), (e) optical microscope images of a flax stem sample under applied torsion, (f) an example of the surface cracking as a result of the torsion, and the image analysis process.

Figure 1a shows pulled flax stems undergoing dew retting in a field. Figure 1b shows a typical bundle of flax stems which were carefully chosen during the study and transported to the laboratory for measurement. Stem samples were gathered weekly for 91 days. Figure 1c shows an example of stem preparation in the laboratory. The dimensions of stem samples were accurately determined using optical microscopy, see Fig. 1d. Figure 1e shows an example of a flax stem under mechanical torsion. This torsion caused a surface stress to be generated along the stem which resulted in characteristic cracking (green arrow) of the stem's outer tissue, see Fig. 1f, which depended on the degree of retting of the stems.

The Retting monitoring tool

Figure 2 shows the original tool which was designed and fabricated to carry out the torsion experiments on the flax stems to test their degree of retting. The following text describes the key parts of the tool and how it is used to conduct the torsion experiments.

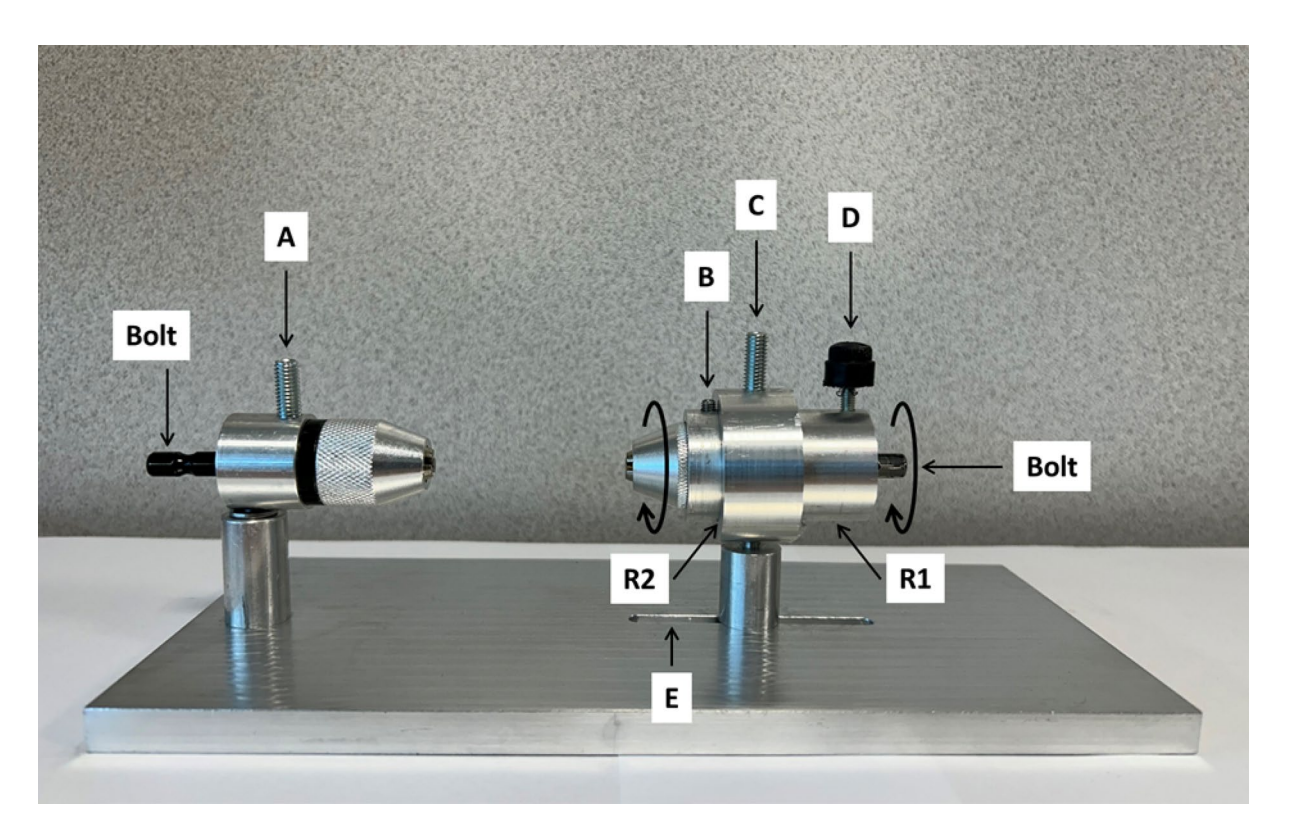


Fig. 2. Photograph of the retting monitoring tool developed for the study.

The tool consists of two self-centring, three-jaw chucks separated by a distance of 50 mm. The left-hand chuck is fixed to the support base plate. The left-hand chuck cannot rotate. The right-hand chuck is also fixed to the support base plate but can slide horizontally and rotate. The right-hand chuck fits inside a hollow metal ring R1 which in turn fits inside a larger outer ring R2 attached to the base plate. The left-hand chuck has a bolt to tighten the chuck jaws and a screw A to block rotation of the chuck. The right-hand chuck has a bolt to tighten the chuck jaws and three screws B, C, and D. Screws B and C can be used to fix the right-hand chuck to the rings; screw D can be used to block the bolt of the right-hand chuck. These locking points ensure that the chuck and bolt are independently fixed once the sample has been firmly gripped, preventing them from twisting separately and eliminating the possibility of sample mounting error. The design ensures secure placement of the stem sample and minimises any potential damage, instability, and slippage of the flax stem during experimentation. Note that the design also allows for eventual buckling of the stem while applying torsion; the right-hand side of the tool can twist and also move laterally to compensate for a length change of the stem due to buckling. This is achieved by allowing ring R1 to move laterally with respect to ring R2 during the measurement. The adjustment gap E enables the flax stem to be inserted without bending, thus avoiding potential damage.

The mounting procedure of a flax stem is as follows. First, the stem is carefully inserted into the left-hand chuck. The left-hand chuck bolt is then tightened until the stem is gripped firmly. Screw A is now tightened to block the left-hand chuck bolt. The right-hand chuck and ring R1 are now moved horizontally to insert the stem into the right-hand chuck jaws. At this moment screws B, C, and D are loose. When the stem length (between the chucks) measures 50 mm, screws B and C are tightened. The bolt on the right-hand chuck is now tightened until the stem is firmly gripped in the right-hand chuck's jaws. At this point, the right-hand bolt is now blocked by tightening screw D. Finally, screw C is now loosened to prime the tool for use. At this point, the bolt of the right-hand chuck can be turned to apply torsion to the stem. The screw C can be tightened at any moment to fix the applied torsion angle. The torsion angle at the right-hand end of the stem can be read off a scale on the tool.

Note that others have characterised plant stems using mechanical torsion²⁰ and it is known that stem gripping by a mechanical chuck is not trivial if one is to avoid damage during the experiment^{21,22}. Not enough force from the chuck leads to slipping and spurious results whereas too much force leads to damage of the stem xylem. We adopted a simple solution to this by wrapping a length of thin latex around the stem ends prior to gripping and developing a know-how concerning the correct bolt-tightening to avoid stem/chuck slipping and damage to the stem xylem.

Measurement protocol

During mechanical testing, the stem surfaces were observed using digital optical microscopy using a VHX-6000 (Keyence, France). There are several advantages gained by using a digital microscope. Image stitching enables large portions of the stems to be characterised at the same time; this enables the identification of local damage which might be missed otherwise. There is a large working distance which enables the mechanical tool to be

placed easily under the microscope objective. The lighting conditions can be strictly controlled and duplicated from one test to another; this enables the identification of damage induced by the mechanical testing from stem to stem. The stem surface is not flat and 3D focusing can be of use. The microscope incorporates in-built image analysis which can be employed in situ for testing. Exact position coordinates are programmable, so that the position of damage can be accurately located along the stem and tracked from measurement to measurement. The resulting microscope images were analysed using software (Keyence, France) and ImageJ²³. Fig. 3 shows the tool being used in the laboratory.

Once the stem is inserted correctly into the tool it is placed under the objective of the digital optical microscope. First, for zero torsion angle, images are taken at fixed positions along the stem. These positions are saved. Next, a torsion angle is applied to the stem and images are taken at the same positions. This procedure is repeated by increasing the torsion angle in steps. The increment of the torsion angle was computed according to the modelling to try to obtain the same surface shear stress increment each time. Note that for different stem diameters, different torsion angles are required to cause comparable surface stresses. During the measurements, the images are analysed for visible damage occurring in the exterior tissue of the stem. In principle, this observational analysis could be achieved by an artificial intelligence (AI) in order to render the whole analysis automatic^{24–26}.

Flax stem sample properties

Prior to the sample mounting, microscope images were taken of the cross-sectional ends of each stem sample to determine the internal and external diameter. A precise knowledge of these dimensions is required for the mechanical modelling to relate the applied torsion angle, the resulting torque, and the induced surface stress. The mechanical modelling also requires accurate knowledge of the shear modulus of the stems. This was accurately determined from separate experiments involving the bending of flax stems to determine the flexural modulus of the stems; (Reda et al., to be published). The average flexural modulus E_f of the stems of the retting period was determined to be 12.8 ± 1.5 GPa. If we consider a Poisson coefficient ν of 0.35^{27} , and in a first approximation the assumption of an isotropic material, then the shear modulus of the stems is of the order of 4.7 ± 0.6 GPa.

Mechanical modelling: determining the torsion-induced surface stress on the stems

We can cause a mechanical torsion in the flax stem by twisting the end of the stem by a torsion angle θ . Depending on the dimensions of the stem and its mechanical properties, this torsion angle will produce a torque T opposing twisting and a maximum shear stress σ_s at the surface of the stem. In order to compute the torsion-induced surface shear stress on the flax stems we can approximate a flax stem to a uniform, thick-walled hollow tube composed of an isotropic material.

For a shaft of uniform cross-section along its length L, the torsion angle θ is given by:

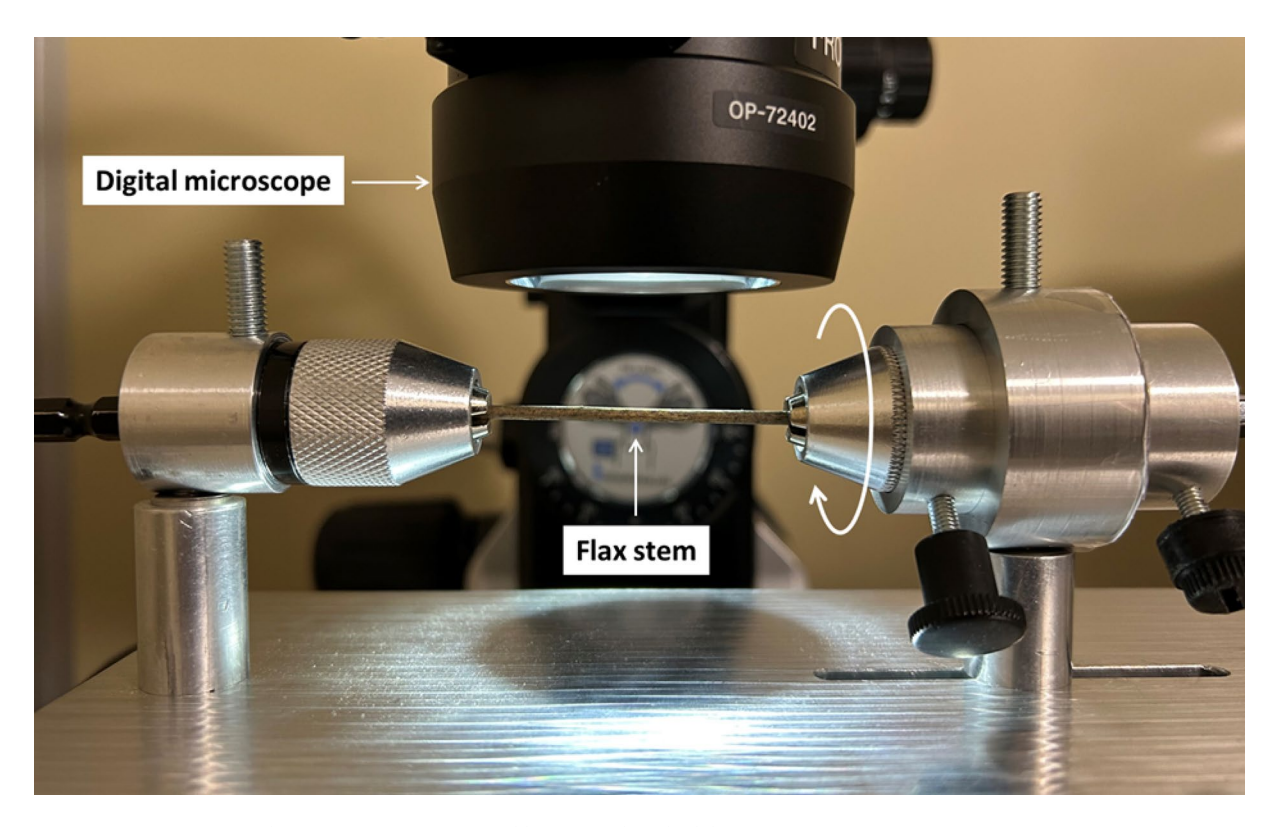


Fig. 3. The retting monitoring tool being used in the laboratory.

$$\theta = \frac{TL}{GI} \tag{1}$$

The shear stress at a point r in a shaft is given by:

$$\sigma_s = \frac{Tr}{J} \tag{2}$$

where J is the torsion constant and the torque T is given by:

$$T = \frac{JG\theta}{L} \tag{3}$$

the shear modulus G is given by:

$$G = \frac{E_f}{2\left(1 + \nu\right)} \tag{4}$$

where E_f and v are the flexural modulus and Poisson ratio of the material. When $r = d_0/2$ (d_0 is the stem's outer diameter) the surface shear stress σ_s is given by:

$$\sigma_s = \frac{E_f \theta \, d_0}{4(1+\nu)L} \tag{5}$$

the torsion constant J of a thick-walled hollow tube is given by:

$$J = \frac{\pi \left(d_o^4 - d_i^4\right)}{32} \tag{6}$$

the torque *J* is therefore given by:

$$T = \frac{\pi \theta}{64L} \left(\frac{E_f}{(1+\nu)} \right) \left(d_o^4 - d_i^4 \right) \tag{7}$$

Equations (5) and (7) are used to compute the surface stress and the torque on the stems from the applied torsion angle.

Experiments and results Under-retted flax stem samples

The optimum retting period was judged by a skilled artisan, Van Robaeys Frères (VRF), to be 56 days (see Methods). Under-retted flax stems were gathered during the period 0–49 days of retting.

Figure 4 shows digital optical microscopy images of an under-retted flax stem sample being subjected to different torsion angles varying from 0 degrees (Fig. 4a) to 110 degrees (Fig. 4d). The images in Fig. 4 show that the stem is correctly fixed. The left-hand end does not rotate while the application of the torsion (white arrows) causes a stem surface feature to rotate, as indicated by the red arrows. Note that the torsion angle reduces from right to left along the stem. However, the torque and the surface stress are, in principle, constant along the stem. To observe the effect of the mechanical torsion on the under-retted flax stem surfaces, zoomed microscopic images were taken as a function of increasing torsion angle.

Figure 5 shows digital optical microscope images of the left end of an under-retted flax stem sample (retting period = 1 day) being subjected to mechanical torsion at torsion angles of 0 degrees (Fig. 5a), 40 degrees (Fig. 5b), 100 degrees (Fig. 5c), and 140 degrees (Fig. 5d).

Figure 6 shows digital optical microscope images of the right end of a flax stem sample (retting period = 49 days) being subjected to mechanical torsion at torsion angles of 0 degrees (Fig. 6a), 50 degrees (Fig. 6b), 100 degrees (Fig. 6c), and 140 degrees (Fig. 6d). This last angle (150 degrees) shows the angle of breaking of the internal tissue of the flax stem. Interestingly, cracks presented by the green arrows appear following a torsion angle of 150 degrees. Several conclusions can be made from the experiments made on under-retted flax stems.

First, before torsion was applied it was observed that all under-retted flax stems demonstrated very little or no visible damaged exterior tissue. It was hypothesised that any visible damage to these stems was not caused by retting. In this study, the epidermis of the flax stems has a light yellow to brown colour for under-retted stems (retting period < 56 days). Note that surface features on the stem allows one to check if the stem is correctly gripped by the two chucks of the tool. In principle, no rotation occurs at the left-hand chuck and the rotation at the right-hand chuck corresponds to the torsion angle.

Second, when torsion was applied to under-retted stems no visible damage in the exterior tissue (epidermis) could be induced by the torsion tool, even at high torque and high surface shear stress in samples (see Figs. 4 and 5). In contrast, cracking can appear in the exterior tissue of some flax stems gathered after 49 days of retting, i.e., 1 week before the optimal retting point— (see Fig. 6c). However, this is not the case of most samples from this retting stage, where in general little visible damage appears in the external tissue following high surface shear stress.

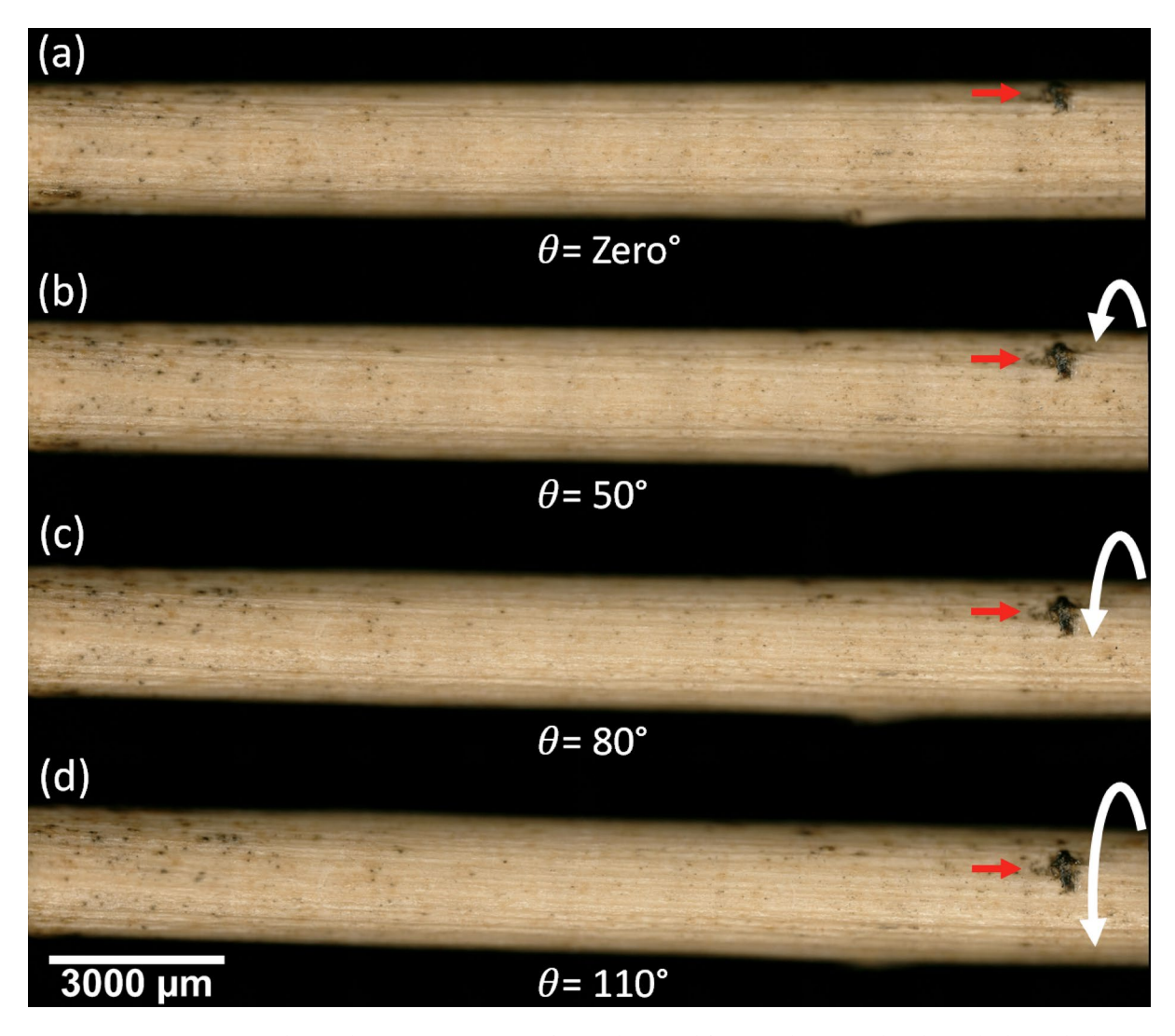


Fig. 4. Digital optical microscope images of an under-retted flax stem being used in the tool. The applied torsion angle is: (**a**) 0 degrees, (**b**) 50 degrees, (**c**) 80 degrees, and (**d**) 110 degrees. The white arrows indicate the torsion. The red arrows indicate the stem surface undergoing rotation.

Third, at a given value of torque it was observed that the inner wood portion (xylem) of the stem broke. By using the modelling, it was observed that this breaking occurred at very similar values of surface shear stress and irrespective of stem diameter. A number of experiments enabled this value to be determined to be 228.24 ± 41.21 MPa for under-retted stems.

Optimally-retted flax stem samples

The optimally-retted flax stem samples were collected on day 56 of retting (see Methods).

Figure 7 shows an example of applying mechanical torsion to a flax stem sample taken from the optimal retting stage as a function of increasing angle; 50 degrees (Fig. 7a), 90 degrees (Fig. 7b), 110 degrees (Fig. 7c), and 150 degrees (Fig. 7d). Figure 7 demonstrates that the left end of the flax stem sample is fixed well to the chuck, demonstrated by the slight buckling effect in the middle of the flax stem sample. This is important to avoid slipping of the sample which results in false results. To better understand the influence of the torsion on the flax stem surface, zoomed microscopic images were taken as a function of increasing torsion angle. Figure 8 shows zoomed optical microscope images of optimally retted flax stems at four different torsion angles.

Figure 8 shows digital optical microscope images of the left (quarter) end of an optimally-retted flax stem sample being subjected to mechanical torsion at torsion angles of 40 degrees (Fig. 8a), 50 degrees (Fig. 8b), 60 degrees (Fig. 8c), and 100 degrees (Fig. 8d). Figure 8 demonstrates that cracks not only appear as a function of increasing torsion angle, but also that the area of these cracks evolve with increasing applied torsion angle which causes increasing torque and surface stress along the stem.

The fact that the surface cracks area evolves as a function of increasing torsion angle and surface stress is an interesting and complex phenomenon which can be studied to understand the functioning of the tool. To better

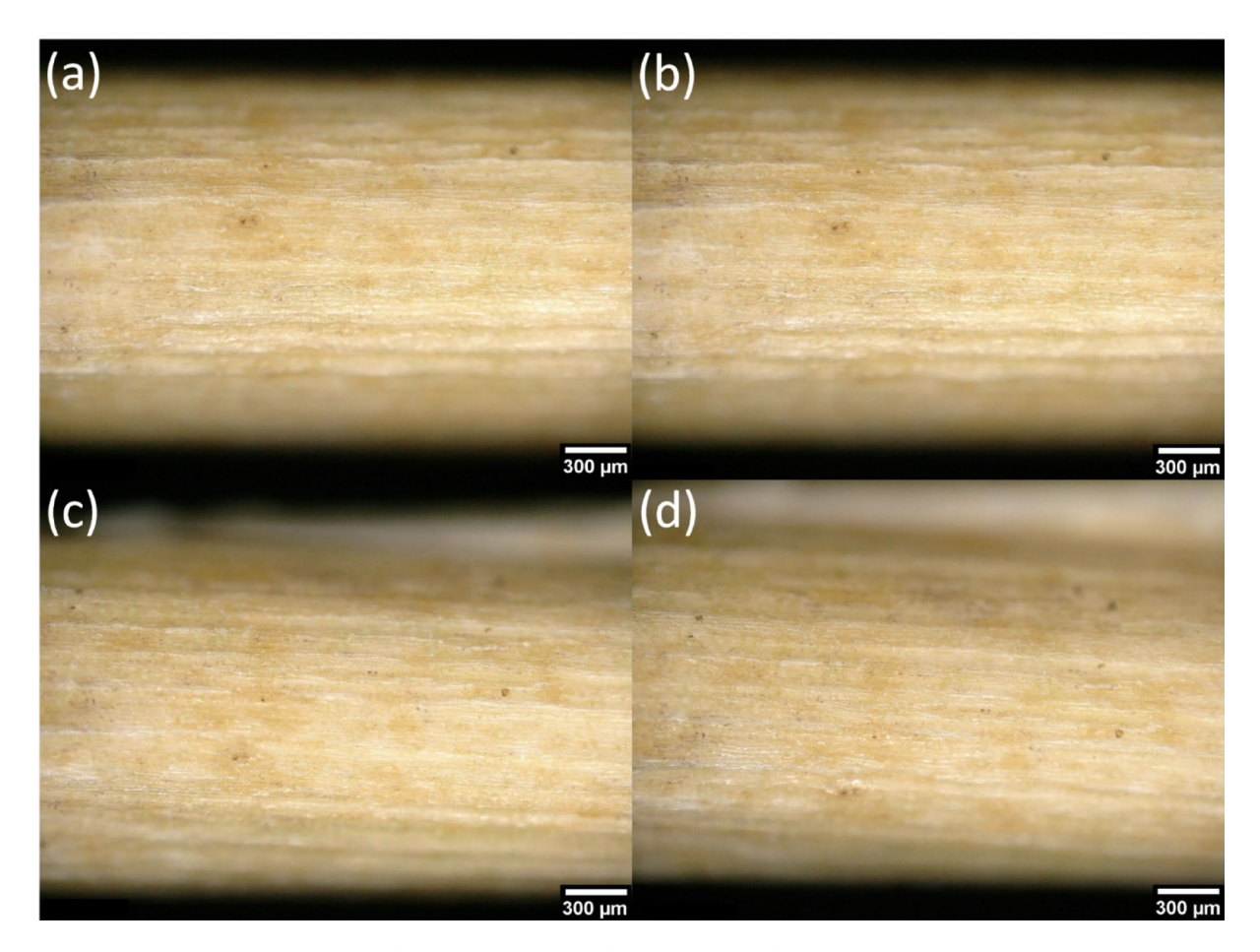


Fig. 5. Zoomed optical microscope images of an under-retted flax stem (retting period = 1 day) being subjected to mechanical torsion. The torsion angles are: (a) 0 degrees, (b) 40 degrees, (c) 100 degrees, and (d) 140 degrees.

understand this phenomenon, the images of surface cracks were processed using image analysis software, and the area was analysed as a function on increasing torsion angle and surface stress.

Figure 9 shows how the torsion-induced surface damage of an optimally-retted flax stem is identified using digital optical microscopy. The top images highlight the creation and evolution of damage in the external stem tissue (green arrows). The middle images show the damage which is identified by the microscope software according to colour (red areas). The bottom images show the identified damage isolated from the stem by removing the background (red areas). The applied torsion angle is 80 degrees (Fig. 9a), 90 degrees (Fig. 9b), and 100 degrees (Fig. 9c). The lower images clearly demonstrate that the total cracking area increases with torsion angle.

Figure 10 shows an example of image analysis of the torsion-induced damage to the exterior tissue of the optimally-retted stem resulting from increasing torsion. Figure 10a-c show the increasing torsion-induced damage image. This torsion angle resulted in damage having different areas that appear, increase in size, and merge. For example, the areas presented by 1 and 2 see (Fig. 10a) evolve to become 4 and 5 see (Fig. 10b), when the torsion angle increases from 80 degrees to 90 degrees. These areas merge together and become one single large crack when the torsion angle increases from 90 degrees as shown in Fig. 10b to 100 degrees as shown in Fig. 10c. Figure 10d plots the evolution of the total damage area as a function of applied torsion angle. This plot shows that the overall cracks area evolution exhibits a linear relation with increasing torsion angle. More examples of results and analysis from the optimally retting stage can be found in the supplementary information. The following observations were made in all optimally-retted samples under torsion.

Over-retted flax stem samples

Over-retted flax stem samples were gathered in the period from 63 days to 91 days of retting (see Methods).

Figure 11 shows optical microscope images of the surface of an over-retted flax stem (retting period = 63 days) being subjected to mechanical torsion. First, it was observed that over-retted flax stems demonstrated a lot of visible damaged exterior tissue. It was hypothesised that the extensive visible damage to these stems was caused by prolonged retting which induces weakening of the epidermis over many parts of the stem epidermis. In this study, the epidermis of the over-retted flax stems has a dark brown/black colour. Again, at a given value of torque it was observed that the inner portion (xylem) of the stem broke. This is the same observation as with the

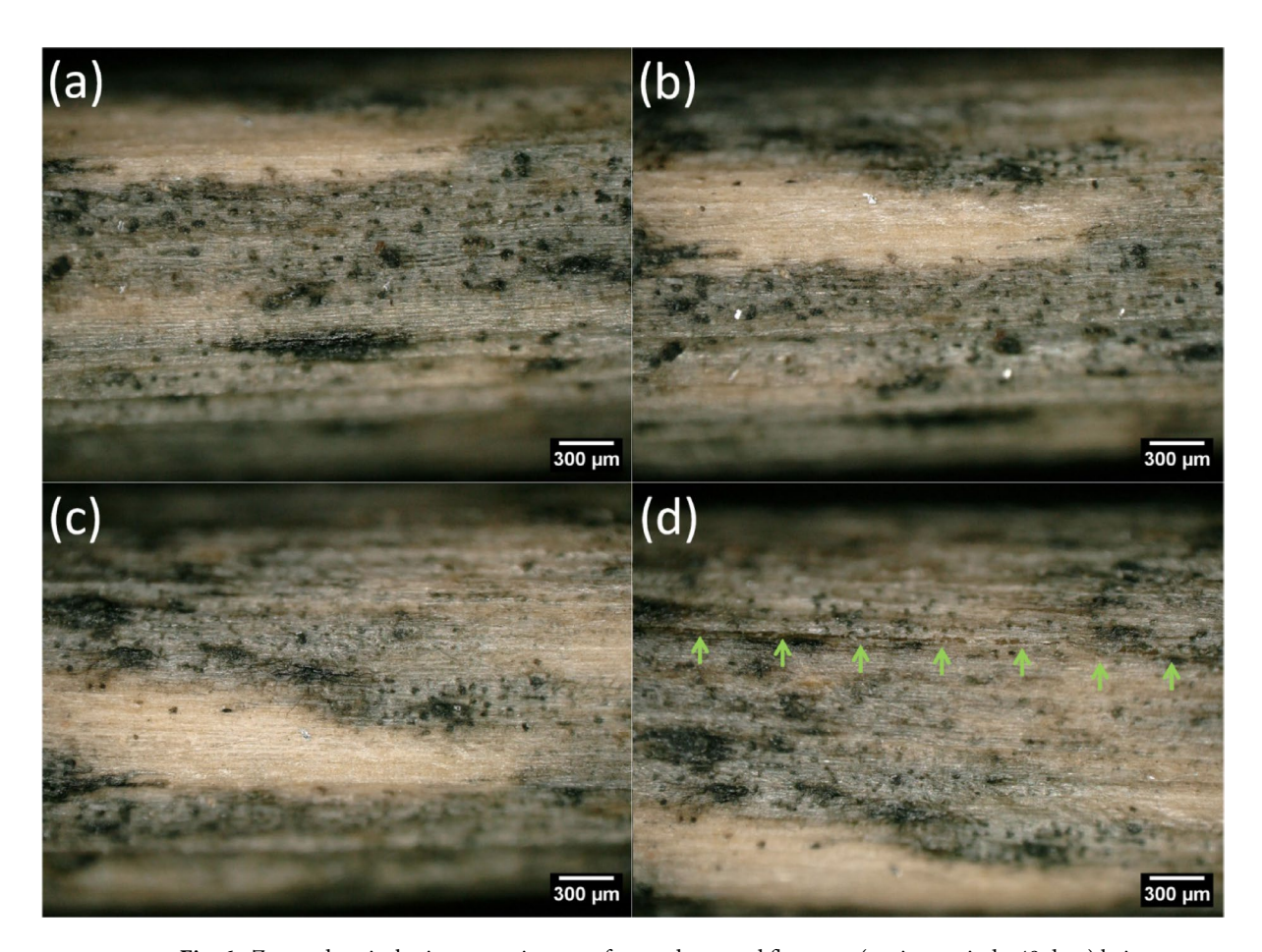


Fig. 6. Zoomed optical microscope images of an under-retted flax stem (retting period = 49 days) being subjected to mechanical torsion. The torsion angles are: (a) 0 degrees, (b) 50 degrees, (c) 100 degrees, and (d) 150 degrees.

under-retted and optimally-retted stems. By using the modelling, it was observed that this breaking occurred at very similar values of surface shear stress, the value was computed to be 253.3 MPa for over-retted stems. This value is very similar to that obtained for under-retted and optimally-retted stems.

Figure 12 shows an example of an over-retted stem gathered at the end of the over-retting period (91 days of retting). The exterior tissue of such stems was already damaged with the fibres being visible.

Discussion

Let us first discuss the potential impact of sample inhomogeneities on the results. There are several causes for inhomogeneities in the stems. First, stems naturally have non-uniform dimensions—we chose apparent uniform stems in the field and validated their uniformity in the laboratory using microscopy. Second, natural damage can occur in retting stems—therefore we carefully chose apparently undamaged stems which were also verified for damage in the laboratory. Third, it is known that the degree of retting can vary across the field—therefore sample gathering was always conducted in a 5 m² part of the field. Fourth, It is known that retting inhomogeneity can occur over time due to position of the stem in the retting pile⁶. This is why the stems are turned during the retting. At the start of retting, samples had a uniform green colour. In contrast, around optimal retting there was a colour variation in the stems which was correlated with the depth in the pile (see Supplementary Information). Therefore, to avoid sampling bias which can affect results, stems samples were taken from different parts of the stem pile (see Methods). For the period near optimum retting, we observed that the stem colour could be correlated with the position in the pile—in general, the bottom stems were darker than the stems at the top of the pile. Despite this colour difference, no observable difference was seen in terms of the mechanical results. In other words, comparable cracking was observed in samples at similar values of applied surface sheer stress.

Figure 13 shows an example of how the stem outer and inner diameters vary along the length of a typical sample. The samples were cut into 1 cm sections to enable several diameter measurements (d1-d6) to be performed using optical microscopy. Note that the outer diameter is relatively constant whereas the inner diameter is less uniform—this is a typical observation of all stem samples tested. For this sample the average outer and inner diameters along the whole sample are $2251.5 \pm 57.5 \, \mu m$ and $1009.9 \pm 60.8 \, \mu m$. The data demonstrate the circularity of the stems and the consistency of the outer diameter along the stem samples taken from the middle

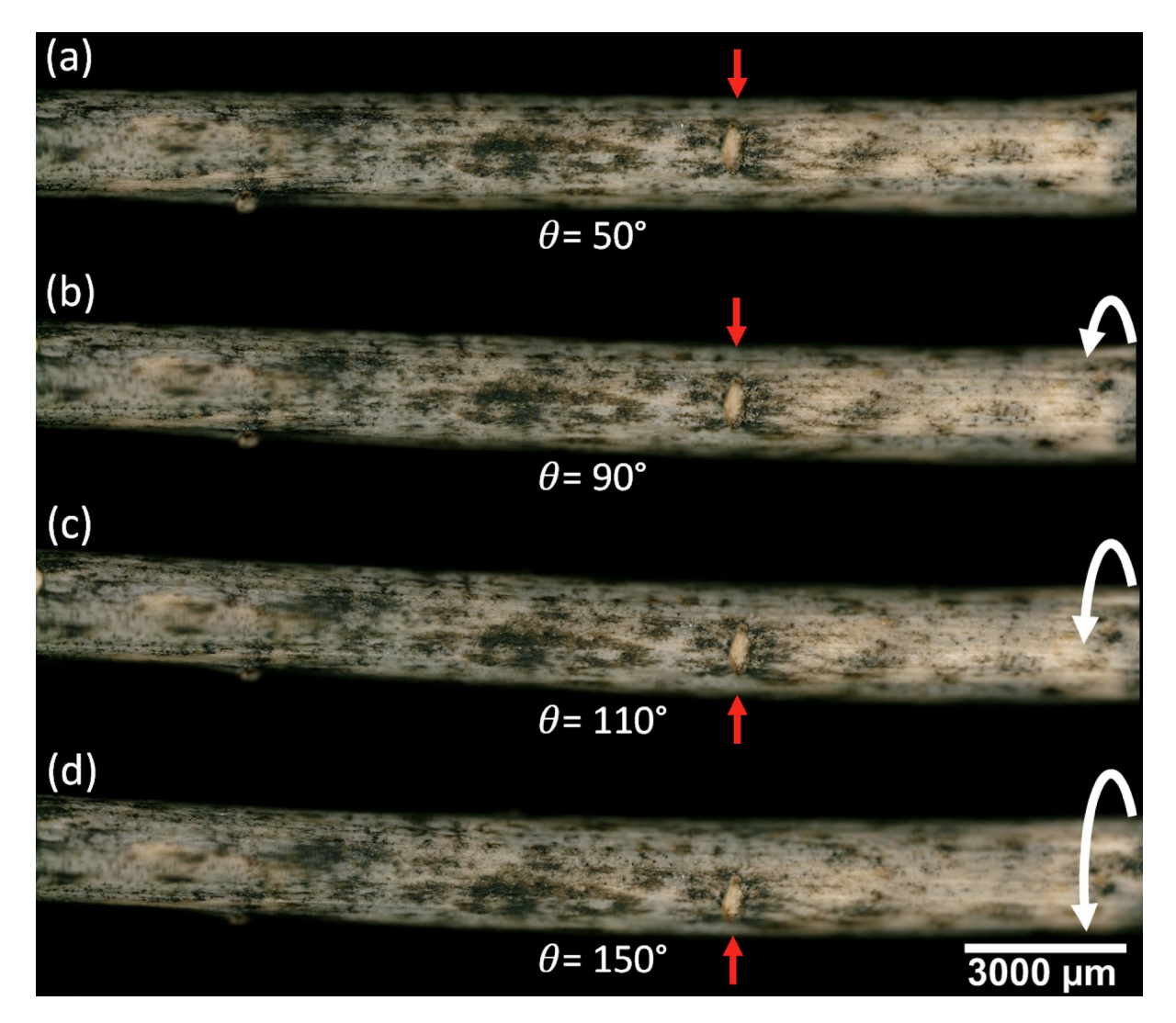


Fig. 7. Digital optical microscope images of an example of an optimally-retted flax stem being used in the tool. The applied torsion angle is: (a) 50 degrees, (b) 90 degrees, (c) 110 degrees, and (d) 150 degrees. The white arrows indicate the application of the torsion angle. The red arrows indicate a stem surface feature undergoing rotation.

of the stalks. As stated above, the modelling (see Mechanical Modelling) is less sensitive to non-uniformity of the inner diameter than the outer diameter.

In terms of the experimental results, when torsion was applied to optimally-retted stems visible damage in the exterior tissue (epidermis) could be induced by the tool. Damage appears initially as small islands—noted by the numbering in the image analysis see (Fig. 10). Increasing the torsion angle increases the surface shear stress along the stem. This causes the damage to increase in size and merge into larger islands. This seems to favour the appearance of long axially-oriented damage which appear to be surface cracks. Note that no radially-oriented cracks were observed. It was observed that the surface shear stress at which the torsion-induced damage occurred was lower than the values of the shear stress required to break the xylem. At a given value of torque it was observed that the inner portion (xylem) of the stem failed. This is the same observation as was made using the under-retted stems. By using the modelling, it was observed that this breaking occurred at very similar values of surface shear stress and irrespective of stem diameter.

Figure 9 shows how image recognition and analysis is performed on the stems as the torsion is applied to the stems using the tool (also see Supplementary Information). For the optimally-retted stems, the torsion and induced surface shear stress causes visible damage in the exterior tissue of the stems. This damage is manually identified by the operator of the tool-although this could be envisaged by being eventually performed by AI. The tool is used to increase the surface shear stress and the evolving damage is recorded at positions along the stem. Once all the data is gathered, image analysis can be used on the data to isolate the torsion-induced damage. In this study, this was done by identifying the colour of the stem that the damage (cracks and patched) revealed. The image analysis was powerful enough to isolate this which enables us to analyse it as a function of increasing shear stress; this is clearly shown on Fig. 9, torsion-induced damage is identified, see upper images.

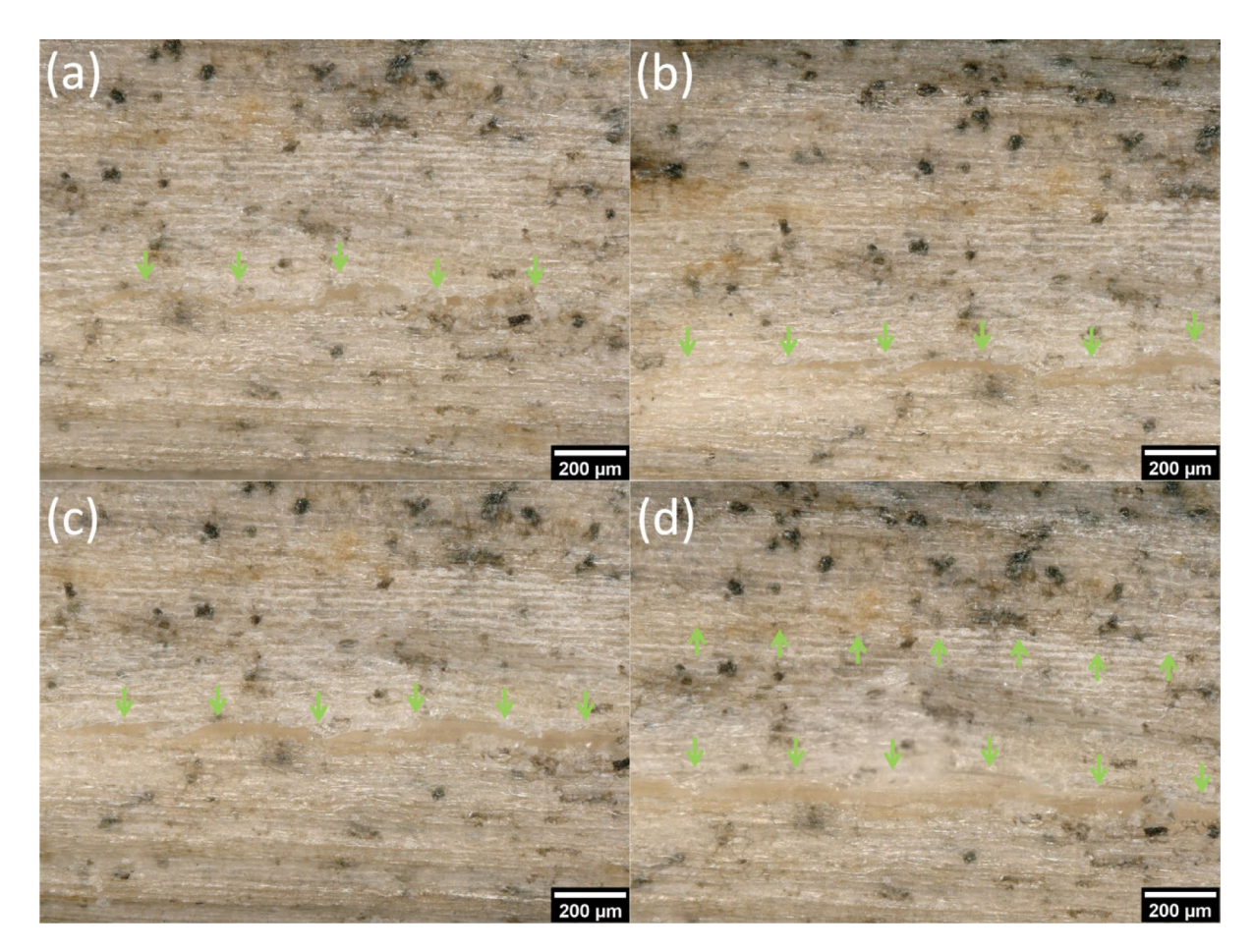


Fig. 8. Zoomed optical microscope images of an optimally-retted flax stem being subjected to torsion. The torsion angles are: (a) 40 degrees, (b) 50 degrees, (c) 60 degrees, and (d) 100 degrees. The torsion-induced damage to the exterior stem tissue is indicated by the green arrows.

The torsion-induced damage is tracked, see middle images, and the damage is isolated for analysis, see lower images. Finally, Fig. 10 shows how the torsion-induced damage was analysed using software. We were able to do this for several stems from the optimally-retted period, as examples; see Supplementary Information. Analysis of this data enabled us to plot how the area of the damage evolved with increasing surface shear stress. The plots show the results of this analysis. This data enables us to estimate a damage evolution factor for optimally-retted stems. Moreover, by using the mathematical modelling given above, it is possible to compare results on several stems. This is done by computing the surface stress on each tested stem sample from the applied torsion angle using Eq. 5. From the image analysis, the torsion-induced damage area can be plotted versus the surface shear stress (see Supplementary Information).

Finally, as with the under-retted stems, image analysis of torsion-induced damage in heavily over-retted stems was not possible. In terms of the tool, this is normal as the tool would not be required to function beyond the optimum retting period.

Summary of mechanical measurements

From the measurements, we were able to determine that the appearance of torsion-induced damage and the stress required to break the xylem in optimally-retted flax to be 96.18 \pm 54.75 MPa and 204.92 \pm 19.55 MPa respectively. In addition, we were able to determine the average shear stress required to break a retted flax stalk independent of the retting stage. This value measures 219.76 \pm 37.97 MPa. Table 1 shows a summary of the main findings of the study.

In-field testing

Previous mechanical approaches

Let us now consider in more detail the mechanical tools that have been developed in the past. In the 1980s, Seaby and Mercer¹¹ developed a mechanical tool to test the degree of retting in flax stems. The tool was able to discern the difference in the force required to collapse the bast and detach the fibres between green (un-retted) and retted flax. A force ratio of 2.2 and 2.5 was observed for bast collapse and fibre detachment respectively. The reasoning behind the tool is that as retting facilitates the mechanical separation of the flax fibres from the stems, then a sufficiently precise mechanical tool should be able to test the degree of retting. Following this, Goodman

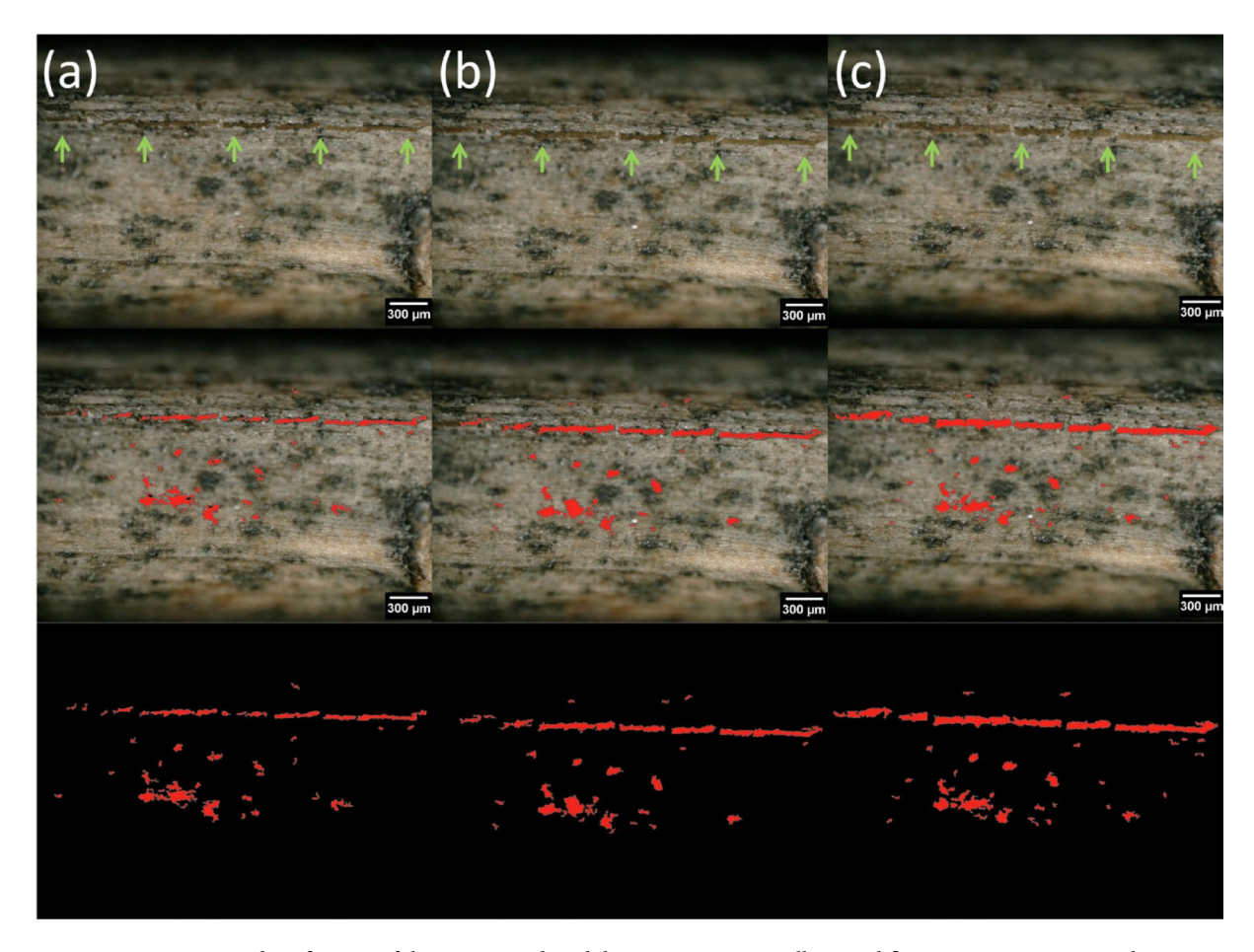


Fig. 9. Identification of the torsion-induced damage in an optimally-retted flax stem using image analysis. The upper images indicate the damage (green arrows). The middle images identify the damage (red areas). The lower images show the isolation of the damage (red areas) ready for analysis. The applied torsion angle is equal to: (a) 80 degrees, (b) 90 degrees, and (c) 100 degrees.

et al. 16 developed another mechanical method to assess the degree of retting of flax stems. Their approach was based on measuring the work required to peel fibre bundles from the secondary phloem tissue. Their reasoning was analogous to that of Seaby and Mercer 11 , in that advancing retting should be visible in the work of peeling. Peeling experiments were followed by tearing experiments. Both approaches observed a correlation between retting and experimentally measured peel and tear work. Booth et al. 17 later modified the approaches developed by Goodman et al. 16 to produce a method capable of monitoring the dew degree of retting in hemp fibre. Their approach measures the work required to remove the outer tissue from the core of the stem. The work of peeling was seen to fall from $\sim 190~{\rm Jm}^{-2}$ to $\sim 100~{\rm Jm}^{-2}$ for 35 days of dew retting. However, the decrease in the work was near linear, and the optimal retting point; was not visible. Réquilé et al. 19 studied the peeling of hemp in different degrees of retting. They observed that peeling experiments can be used to monitor the reduction in energy required to extract fibre bundles from hemp stems. They concluded that peeling could therefore be used to monitor the degree of retting of bast fibre stems such as hemp and flax. Martin et al. 28 found that the degree of retting was visible in tensile testing of flax fibres.

The prototype tool

Figure 14 shows how a portable tool can be used 'in-the-field' during a flax retting period. First, a single tool could be used once a day by an operator who performs tasks very similar to those of our laboratory tests. One could also envisage multiple tools being used by several operators gathering data in several fields. Going further, one could imagine a fully-automated motorised tool where the tool is left in the field and the torsion is applied remotely by a wireless network. The data could be sent via a wireless link and analysed (possibly using AI) remotely to access the degree of retting in real time. In this case, torque sensors could be added to the device to accurately control the applied surface stress. A weather station could also be integrated into the wireless set up. This enables the tool to be used in the correct condition, e.g., dry stems.

Figure 15 shows a flow diagram on how the tool should be used. Damage-free flax stems should be collected weekly throughout the retting process. From each stem, a 7 cm long segment is cut from the central, morphologically homogeneous portion. The external diameter of each segment is measured using a micrometer to ensure a constant diameter stem sample. The sample is then inserted into a prototype torsion testing apparatus.

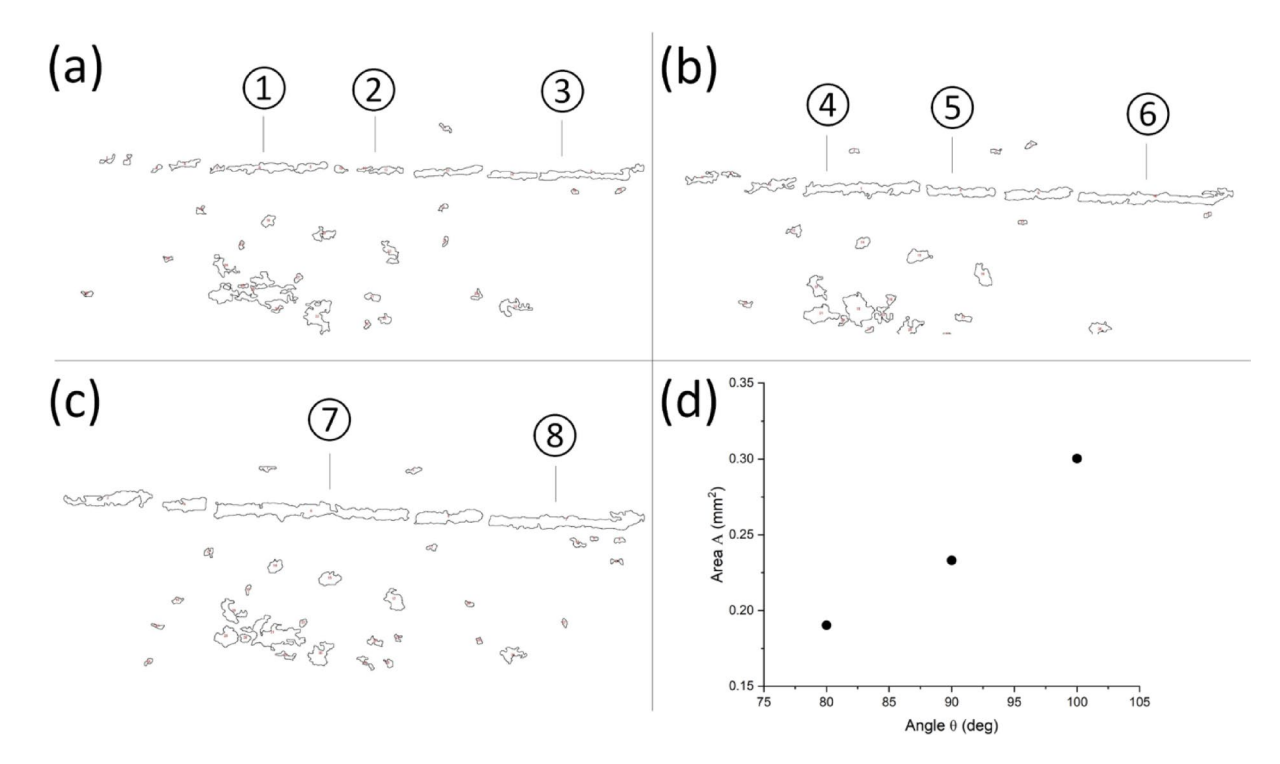


Fig. 10. Analysis of the torsion-induced surface damage in optimally-retted flax stems. Induced surface damage for an applied torsion angle equal to: (a) 80 degrees, (b) 90 degrees, and (c) 100 degrees. (d) Plot showing the variation of total damage area as a function of torsion angle.

Based on the measured stem diameter, a predefined torsion angle—extracted from a reference lookup table established in this scientific study—is applied. This angle corresponds to the expected cracking threshold under conditions of optimal retting. If the applied torsion does not induce cracking, retting is continued. If cracking occurs, retting can be considered complete and is terminated. When the retting is complete, the observed cracking is very distinctive. Therefore, in principle only one sample is required. However, artisanal testing in the field uses multiple samples, we therefore suggest testing a selection of samples, as is the case for the artisanal method.

Conclusions

Combining mechanical methods, digital optical microscopy, and image analysis has proved to be successful to produce a prototype smart tool capable of monitoring the degree of dew retting of flax stems. Cracking of the outer tissue of retting flax stems, due to applied mechanical torsion generating a surface stress, can be used as an indicator to identify the optimal dew retting stop point of retting flax stems. The results revealed that a critical surface stress causes cracking only the external tissue of optimally-retted flax stems. The study suggests that a reliable portable in-the-field smart tool to monitor the degree of retting is feasible. The authors note that artificial intelligence (AI) could be used to better identify the amount of damage in the external tissue. In this way a more accurate prediction of the optimal retting stopping point could be obtained than by human judgement. This original approach has the potential to improve natural fibre production in other crops by stimulating research in this area. Note that the original findings here are based on a single retting cycle which has enabled the demonstration of a prototype tool, further studies would enable the development of a reliable commercial tool.

Methods Sample gathering

Retted flax stem samples were collected from a field run by the Van Robaeys Frères company (VRF) located near Killem in the north of France. The flax stem samples were collected during summer/autumn 2022. The sample gathering lasted 91 days from the 6th of July until the 4th of October. The flax stems were: Family: *Linaceae*, Genus: *Linum*, Species: *L. Usitatissimum*, Variety: *Felice*. The weather during the course of the retting period can be found in the Supplementary Information. Two samplings were conducted per week (Monday and Thursday); stems were taken from the field between midday and 2pm. Stems were taken from the same part of the field each time. The designated sampling area in the field was 5 m². The stems were taken from the bottom, middle, and top of the stem pile each time. The stem pile height was typically 5 cm. Visibly unbroken and undamaged stems were selected as test samples. Uniform stems were chosen as test samples, they had diameters in the range 1–3 mm. The stem sample lengths were typically 35 cm. The stems were carefully transported to the laboratory (70 km) to avoid mechanical damage. In the case of wet samples due to rainfall, it has been shown the stem samples require a minimum 4 h drying to achieve a stable room temperature moisture content before they can

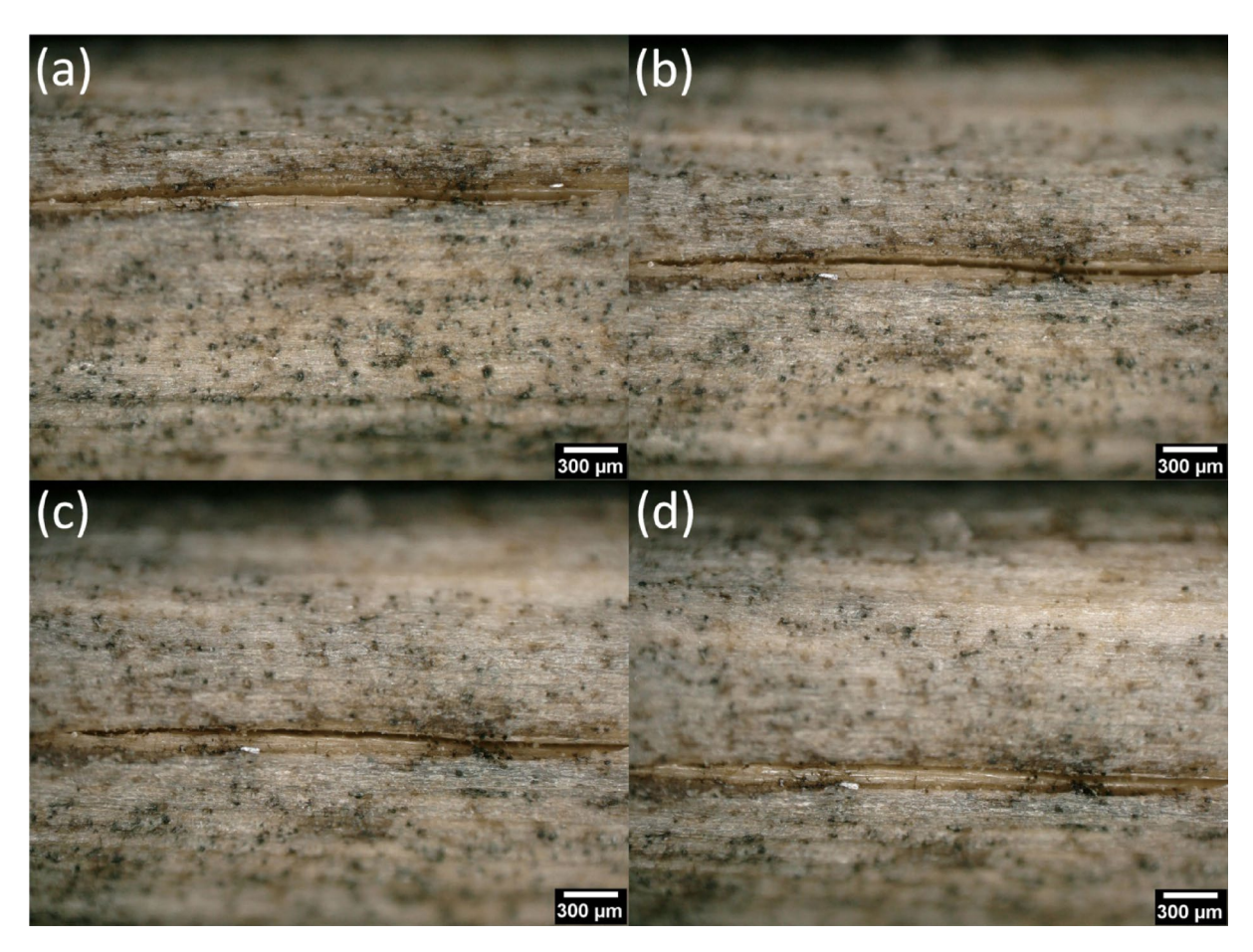


Fig. 11. An example of an over-retted flax stem being subjected to increasing mechanical torsion. The torsion angle is (a) 20 degrees, (b) 50 degrees, (c) 80 degrees, and (d) 100 degrees. This sample spent 63 days retting in the field.

be tested by the tool²⁹. Independently from our study, the optimum retting period of the stems was judged by a skilled artisan (VRF) to be 56 days. At this time, most of the flax stems were gathered using machinery for storage and eventual industrial fibre extraction. However, to enable our study to span 91 days of retting (under retting, optimum retting, and over retting) VRF allowed us to keep several square metres of retting stems in the field. We can therefore classify under-retted stems (0–55 days), optimally-retted stems (56 days), and over-retted stems (57–91 days).

Sample preparation

The experiments required uniform, 70 mm-long stem samples. The samples prepared for the experiments were exclusively taken from the middle portion of the flax stalk, where the diameter is most homogenous, as was observed in this study (small variation of diameter). The cutting of stem samples was done in a way so as to not crush the stem ends; it was anticipated that this could propagate damage and affect experimental results. Minimally-damaged stem ends were achieved using a metal block (with different hole diameters) to hold the stem in place and a sharp razor blade to cut the stem. Note that good quality ends of the stems also enabled optical microscopy to be performed to access the outside and inside diameters at each stem; this enables stem uniformity to be determined and also enables mechanical modelling based on these parameters. Following testing, the stems were further cut using the same means to measure stem uniformity and diameter (outer and inner) along the stem.

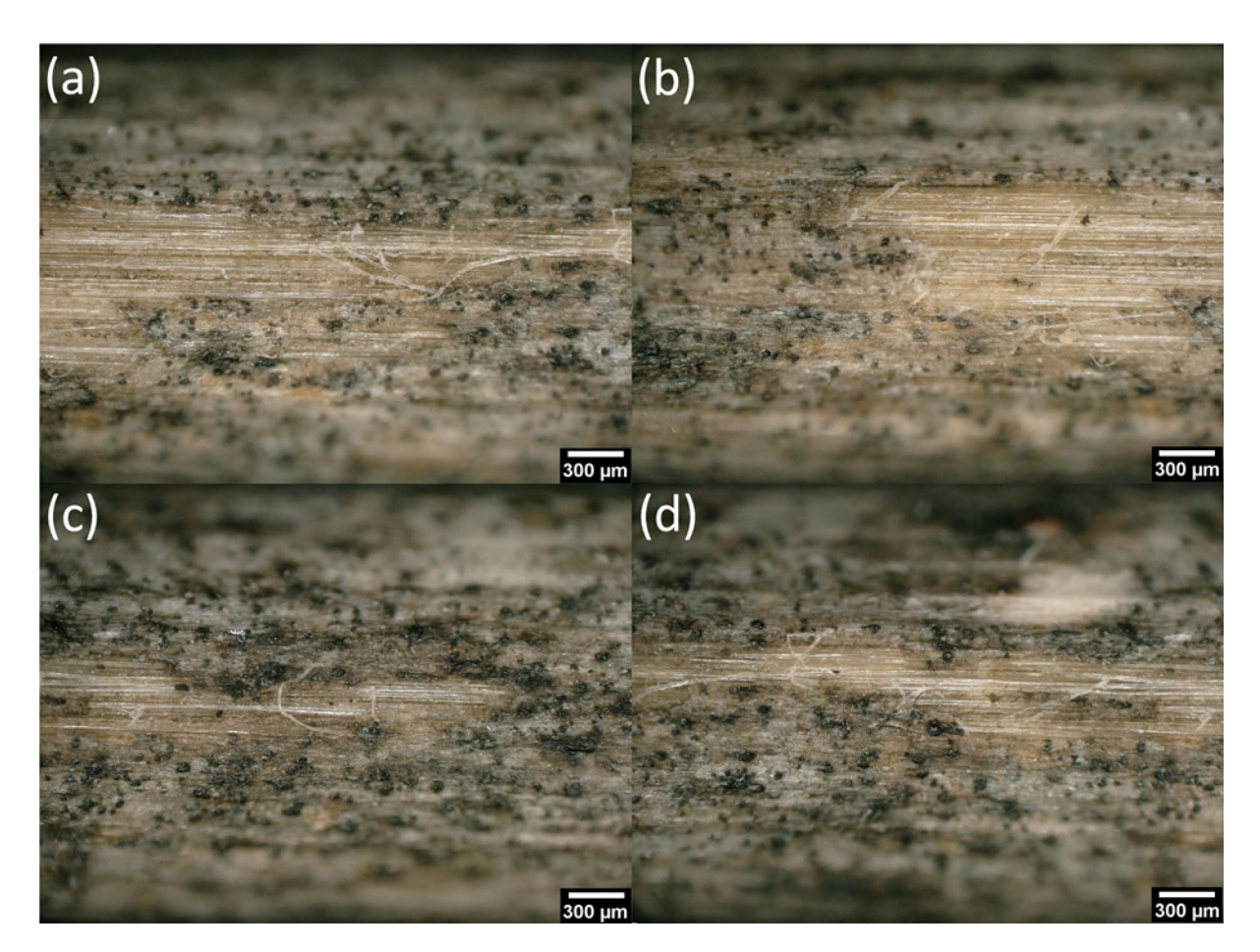
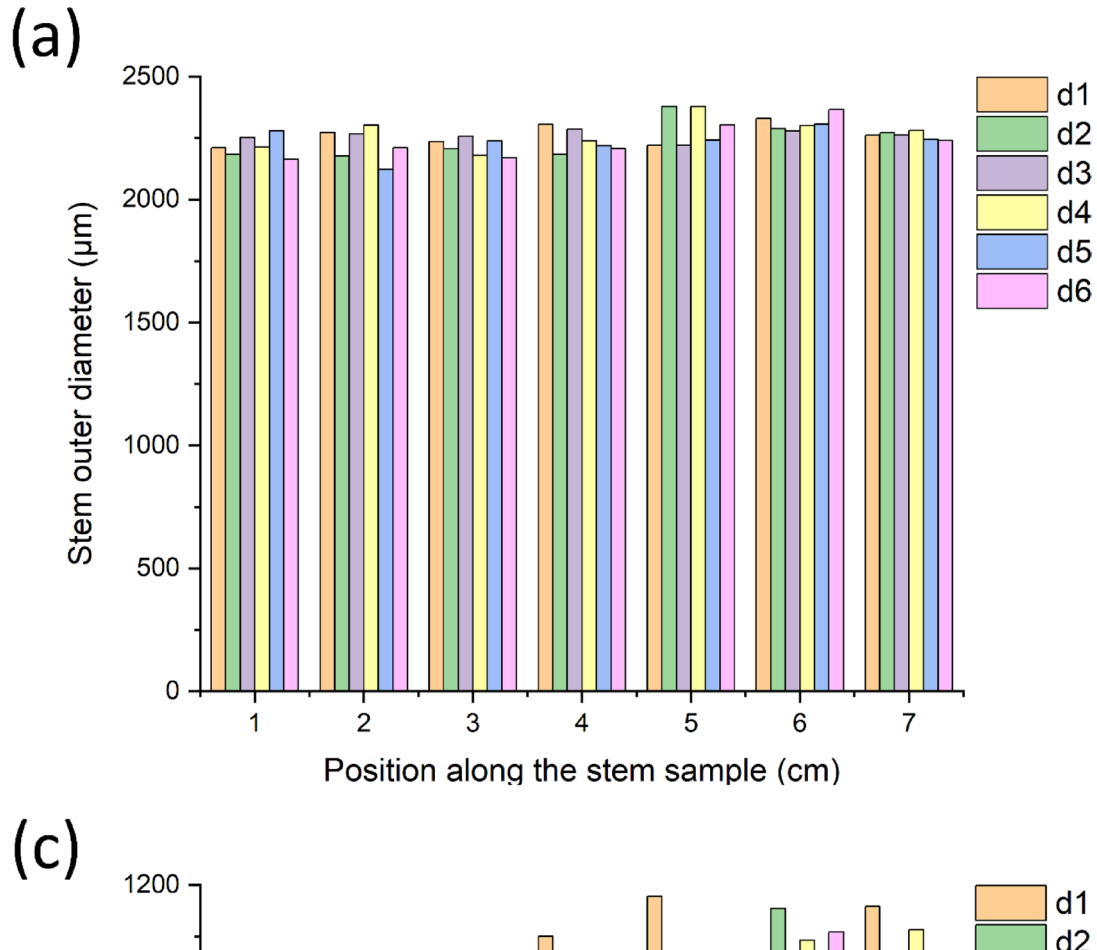


Fig. 12. An example of an extreme over-retted flax stem gathered at the end of the over-retting period (91 days of retting).



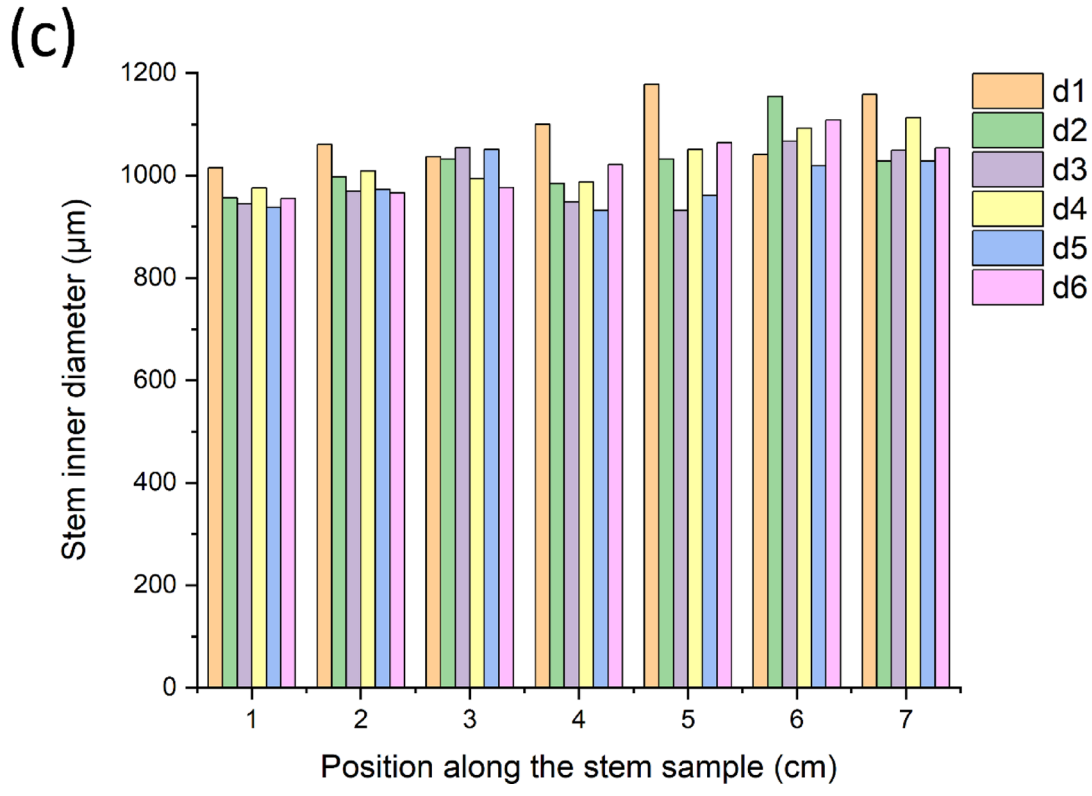
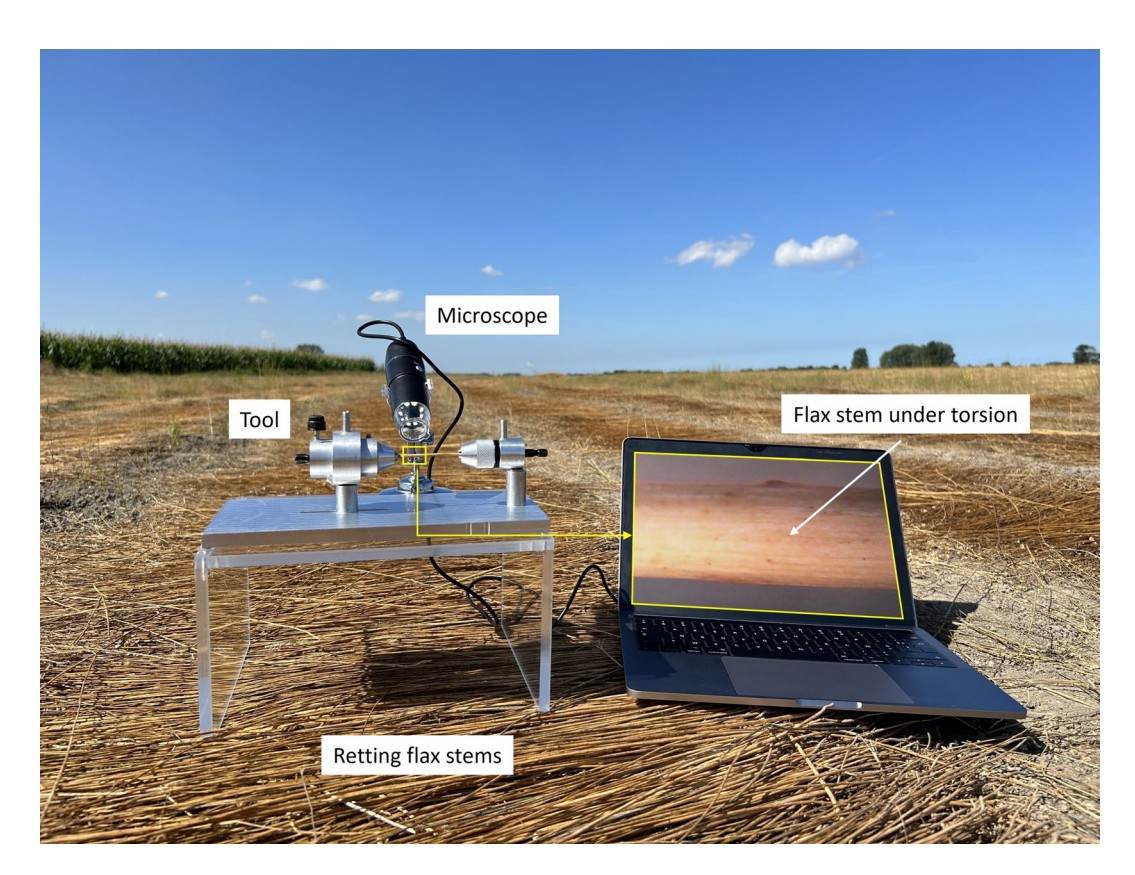


Fig. 13. An example of the variation of (a) outer diameter and (b) inner diameter along the stem sample. Six measurements are taken at each cross-section, cross-sections are cut in centimetre intervals.

Measured property	Surface shear stress σ_s (MPa)
Average Surface shear stress σ_{s} to cause visible damage in optimally-retted flax stems	96.18 ± 54.75
Average Surface shear stress σ_{s} to break the xylem of optimally-retted flax stems	204.92 ± 19.55
Average Surface shear stress σ_{s} to break the xylem of all flax stems	219.76 ± 37.97

Table 1. Summary of the mechanical properties of the flax stems measured in the study.



 $\label{Fig. 14.} \textbf{The retting monitoring tool being used in the field.}$

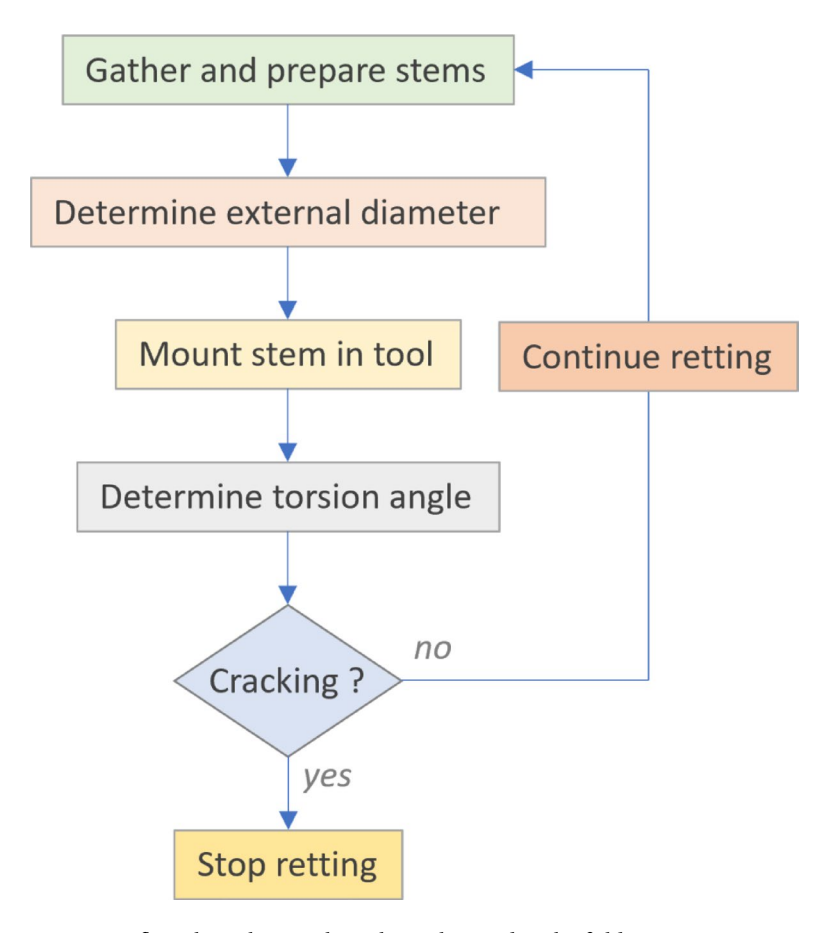


Fig. 15. A flow chart showing how the tool is used in the field.

Data availability

The datasets used during the current study are available from A.R. (ali.reda@univ-lille.fr) and S.A. (steve.arscott@univ-lille.fr) on reasonable request.

Received: 28 March 2025; Accepted: 21 July 2025

Published online: 14 October 2025

References

- 1. Jhala, A. & Hall, L. Flax (Linum usitatissimum L.): current uses and future applications. *Aust J. Basic. Appl. Sci.* 4, 4304–4312 (2010).
- 2. Yan, L., Chouw, N. & Jayaraman, K. Flax fibre and its composites A review. Compos. Part. B: Eng. 56, 296-317 (2014).
- 3. Md. Tahir, P., Ahmed, A. B., SaifulAzry, S. O. A. & Ahmed, Z. Retting process of some Bast plant fibers and its effect on fibre quality: A review. *BioRes* 6, 5260–5281 (2011).
- 4. Åkin, D. E. Linen most useful: Perspectives on structure, chemistry, and enzymes for retting flax. *I 2013SRN Biotechnol.* **2013**, 1–23 (2013).
- 5. Lee, C. H., Khalina, A., Lee, S. H. & Liu, M. A. Comprehensive review on bast fibre retting process for optimal performance in fibre-reinforced polymer composites. *Adv. Mater. Sci. Eng.* **2020**, 6074063 (2020).
- Angulu, M. & Gusovius, H. J. Retting of Bast fiber crops like hemp and Flax—A review for classification of procedures. Fibers 12, 28 (2024).
- 7. Beijerinck, M. W. (ed van Delden, A.) On the bacteria which are active in flax-rotting. Proc. R Neth. Acad. Arts Sci. 6 462–481 (1904).
- 8. Pallesen, B. E. The quality of combine-harvested fibre flax for industrials purposes depends on the degree of Retting. *Ind. Crops Prod.* 5, 65–78 (1996).
- 9. Davis, R. Flax-Stem Anatomy in Relation to Retting 27 (1923).
- 10. Fraser, T. W., Courtney, A. D. & Harvey, B. M. R. Pre-harvest Retting of flax: a light microscope study of the effects of glyphosate treatment on the maturation of stem tissues. *Ann. Appl. Biol.* 101, 533–537 (1982).
- 11. Seaby, D. A. & Mercer, P. C. Development of a hand tool to test the degree of Retting of flax straw. Ann. Appl. Biol. 104, 567–573 (1984).
- 12. Meijer, W. J. M., Vertregt, N., Rutgers, B. & Van De Waart, M. The pectin content as a measure of the Retting and rettability of flax. *Ind. Crops Prod.* 4, 273–284 (1995).
- 13. Henriksson, G. et al. Identification and Retting efficiencies of fungi isolated from dew-retted flax in the united States and Europe. *Appl. Environ. Microbiol.* **63**, 3950–3956 (1997).
- 14. Fila, G., Manici, L. M. & Caputo, F. In vitro evaluation of dew-retting of flax by fungi from Southern Europe. *Ann. Appl. Biol.* 138, 343–351 (2001).

- Sharma, H. S. S. & Reinard, N. Evaluation of visible and Near-Infrared spectroscopy as a tool for assessing fiber fineness during mechanical Preparation of Dew-Retted flax. Appl. Spectrosc. 58, 1431–1438 (2004).
- Goodman, A. M., Ennos, A. R. & Booth, I. A mechanical study of Retting in glyphosate treated flax stems (Linum usitatissimum). Ind. Crops Prod. 15, 169–177 (2002).
- 17. Booth, I., Goodman, A. M., Grishanov, S. A. & Harwood, R. J. A mechanical investigation of the Retting process in dew-retted hemp (Cannabis sativa). *Ann. Appl. Biology.* **145**, 51–58 (2004).
- 18. Waldron, D. & Harwood, J. A preliminary investigation into the influence of chemical composition on the dynamic mechanical properties of flax (*Linum usitattisimum*) straw. *J. Nat. Fibers.* 8, 126–142 (2011).
- 19. Réquilé, S., Le Duigou, A., Bourmaud, A. & Baley, C. Peeling experiments for hemp Retting characterization targeting biocomposites. *Ind. Crops Prod.* 123, 573–580 (2018).
- 20. Shah, D. U., Reynolds, T. P. & Ramage, M. H. The strength of plants: theory and experimental methods to measure the mechanical properties of stems. *J. Exp. Bot.* **68**, 4497–4516 (2017).
- 21. Wright, C. T. et al. Biomechanics of wheat/barley straw and corn Stover. Appl. Biochem. Biotechnol. 121, 5-19 (2005).
- 22. Zeng, X., Mooney, S. J. & Sturrock, C. J. Assessing the effect of fibre extraction processes on the strength of flax fibre reinforcement. Compos. Part A: Appl. Sci. Manufac. 70, 1–7 (2015).
- 23. Schindelin, J. et al. Fiji: an open-source platform for biological-image analysis. Nat. Methods. 9, 676-682 (2012).
- Akkem, Y., Biswas, S. K. & Varanasi, A. Smart farming using artificial intelligence: A review. Eng. Appl. Artif. Intell. 120, 105899 (2023).
- 25. Islam, M. et al. Destructive and non-destructive measurement approaches and the application of AI models in precision agriculture: a review. *Precision Agric.* 25, 1127–1180 (2024).
- 26. Holzinger, A., Fister, I., Fister, I., Kaul, H. P. & Asseng, S. Human-Centered AI in smart farming: toward agriculture 5.0. IEEE Access. 12, 62199–62214 (2024).
- 27. Kretschmann, D. The Mechanical Properties of Wood 5-46 https://www.fs.usda.gov/research/treesearch/37427 (2010).
- 28. Martin, N., Mouret, N., Davies, P. & Baley, C. Influence of the degree of Retting of flax fibers on the tensile properties of single fibers and short fiber/polypropylene composites. *Ind. Crops Prod.* 49, 755–767 (2013).
- 29. Reda, A., Buchaillot, L. & Arscott, S. Drying behavior of flax stems at different degrees of dew Retting under simulated rainfall: implications for smart agriculture and sensor development. *Agriculture* 15, 395 (2025).

Acknowledgements

The authors would like to thank Pierre d'Arras and Nicolas Ryckeboer from the Van Robaeys Frères company (Killem, France) for allowing us to collect flax stem samples from their fields and practical help. The authors thank Sébastien Grec and Suvajit Mukherjee (UGSF-CNRS-Université de Lille) for supplying sample gathering tools and equipment. We also thank Sébastien Grec (UGSF-CNRS-Université de Lille) for liaising with Van Robaeys Frères to enable sample gathering. The authors thank the CNRS for funding the 80 Prime 'VAL project' and for the PhD funding of AR.

Author contributions

A.R. and S.A. gathered and prepared the samples. A.R. and S.A. designed and performed the experiments, derived the models and analysed the data. All authors provided input for the design of the mechanical tool. J-M. M. fabricated the mechanical tool. L.B. obtained project funding. S.A. and L.B. directed the project. A.R. and S.A. wrote the manuscript. All authors reviewed and corrected the manuscript.

Declarations

Competing interests

The authors declare no competing interests.

Ethical approval

The authors acknowledge that they have complied with all relevant institutional, national, and international guidelines and legislation concerning the IUCN policy statement on research involving species at risk of extinction and the convention on the trade in endangered species of wild fauna and flora.

Additional information

Supplementary Information The online version contains supplementary material available at https://doi.org/1 0.1038/s41598-025-12801-1.

Correspondence and requests for materials should be addressed to S.A.

Reprints and permissions information is available at www.nature.com/reprints.

Publisher's note Springer Nature remains neutral with regard to jurisdictional claims in published maps and institutional affiliations.

Open Access This article is licensed under a Creative Commons Attribution-NonCommercial-NoDerivatives 4.0 International License, which permits any non-commercial use, sharing, distribution and reproduction in any medium or format, as long as you give appropriate credit to the original author(s) and the source, provide a link to the Creative Commons licence, and indicate if you modified the licensed material. You do not have permission under this licence to share adapted material derived from this article or parts of it. The images or other third party material in this article are included in the article's Creative Commons licence, unless indicated otherwise in a credit line to the material. If material is not included in the article's Creative Commons licence and your intended use is not permitted by statutory regulation or exceeds the permitted use, you will need to obtain permission directly from the copyright holder. To view a copy of this licence, visit http://creativecommons.org/licenses/by-nc-nd/4.0/.

© The Author(s) 2025